Published in "ACS Nano 13(6): 6790–6800, 2019" which should be cited to refer to this work.

Polymer-Coated Gold Nanospheres Do Not Impair the Innate Immune Function of Human B Lymphocytes *in Vitro*

Sandra Hočevar,[†,‡] Ana Milošević,[†,#] Laura Rodriguez-Lorenzo,[†,⊗] Liliane Ackermann-Hirschi,[†] Ines Mottas,[‡,§] Alke Petri-Fink,[†] Barbara Rothen-Rutishauser,[†] Carole Bourquin,[*,‡,§,∥,∇] and Martin James David Clift[*,†,⊥,∇]

[†]BioNanomaterials, Adolphe Merkle Institute, University of Fribourg, 1700 Fribourg, Switzerland
[‡]School of Pharmaceutical Sciences, University of Geneva, University of Lausanne, 1211 Geneva, Switzerland
[§]Chair of Pharmacology, Faculty of Science and Medicine, University of Fribourg, 1700 Fribourg, Switzerland
[∥]Faculty of Medicine, University of Geneva, Rue Michel-Servet 1, 1211 Geneva, Switzerland
[⊥]In Vitro Toxicology Group, Swansea University Medical School, Wales SA2 8PP, U.K.

Supporting Information

ABSTRACT: **Gold nanoparticles (GNPs) are intended for use within a variety of biomedical applications due to their physicochemical properties. Although, in general, biocompatibility of GNPs with immune cells such as macrophages and dendritic cells is well established, the impact of GNPs on B lymphocyte immune function remains to be determined. Since B lymphocytes play an important role in health and disease, the suitability of GNPs as a B cell-targeting tool is of high relevance. Thus, we provide information on the interactions of GNPs with B lymphocytes. Herein, we exposed freshly isolated human B lymphocytes to a set of well-characterized and biomedically relevant GNPs with distinct surface (polyethylene glycol (PEG), PEG/poly(vinyl alcohol) (PEG/PVA)) and shape (spheres, rods) characteristics. Polymer-coated GNPs poorly interacted with B lymphocytes, in contrast to uncoated GNPs. Importantly, none of the GNPs significantly affected cell viability, even at the highest concentration of 20 μg/mL over a 24 h suspension exposure period. Furthermore, none of the nanosphere formulations affected the expression of activation markers (CD69, CD86, MHC II) of the naive B lymphocytes, nor did they cause an increase in the secretion of pro-inflammatory cytokines (*i.e.* , IL-6, IL-1β). However, the absence of polymer coating on the sphere GNPs and the rod shape caused a decrease in IL-6 cytokine production by activated B lymphocytes, suggesting a functional impairment. With these findings, the present study contributes imperative knowledge toward the safe-by-design approaches being conducted to benefit the development of nanomaterials, specifically those as theranostic tools.**

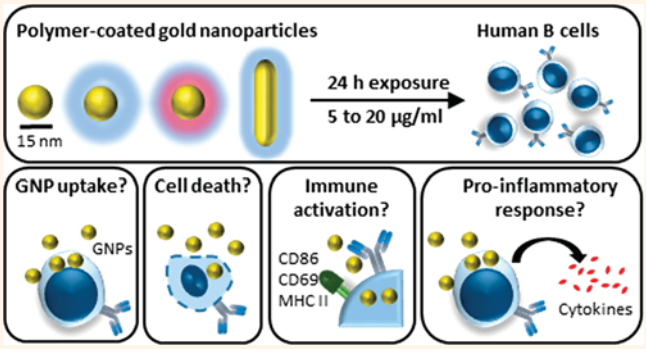

KEYWORDS: *gold nanoparticles, B lymphocytes, nanotoxicology, innate immunity, antigen-presenting cells*

B lymphocytes, often referred to as B cells, are an important subpopulation of immune cells that are found throughout the body in the blood and lymphoid organs. As the sole producers of antibodies, they are essential effectors of protective immunity against infections. B cells also regulate the function of other immune cells, such as T lymphocytes, by presenting processed antigens *via* the major histocompatibility complex (MHC) and by secreting various cytokines that act as immune mediators. In pathological conditions, B cell dysfunction can lead to diseases such as allergy, autoimmunity or cancer.[1] Because of their critical role in health and disease, B cells have generated increased interest in recent years as a target for drug delivery. Indeed, B cells have been successfully targeted by 80 nm lipid nanoparticles (NPs) carrying vaccines against influenza, HIV or Zika virus, or immunotherapies against allergic diseases.[2−4] Despite these recent advances, the direct impact of NPs on B lymphocytes is still poorly understood. Importantly, B cells can respond in an

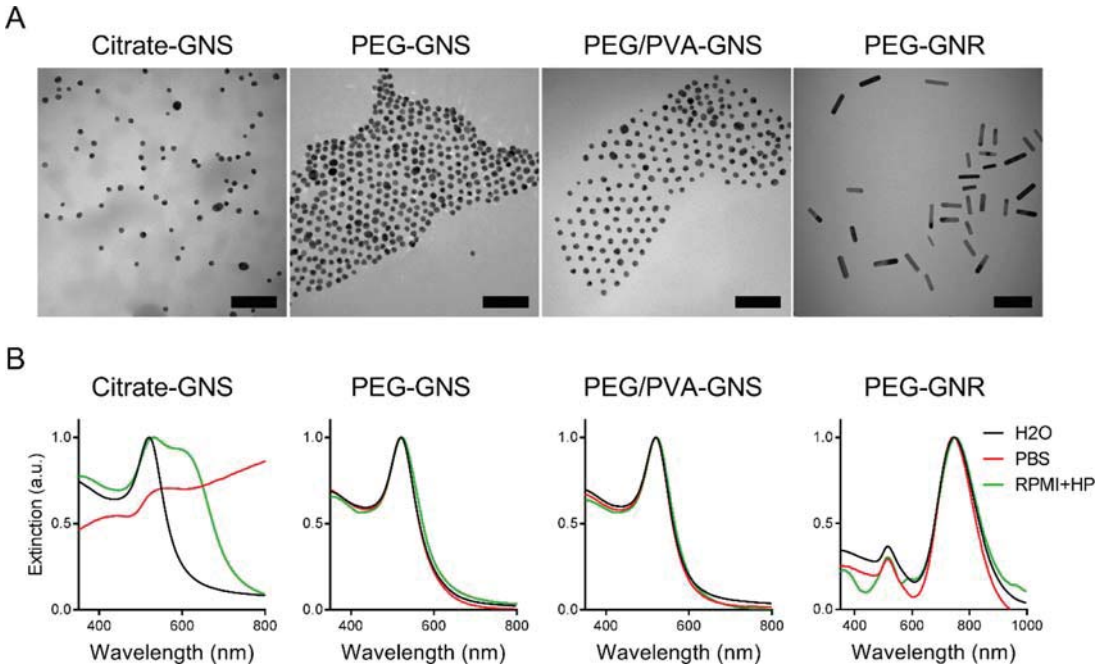

Figure 1. Characterization of gold nanoparticles (GNPs). (A) Representative TEM images of citrate-stabilized gold nanospheres (Citrate-GNS), gold nanospheres with a polyethylene glycol polymer coating (PEG-GNS), gold nanospheres with a combination of PEG and PVA polymer coating (PEG/PVA-GNS), and gold nanorods with PEG coating (PEG-GNR) in H_2O. Scale bars: 100 nm. (B) UV−vis spectra of GNPs in different biological media. Each spectrum was normalized relative to their maximum wavelength. RPMI + HP: complete culture medium consisting of Roswell Park Memorial Institute 1640 with 1% penicillin/streptomycin, 1% L-glutamine, and 10% human plasma.

Table 1. Characterization of Gold Nanoparticle Size and Surface Charge in Complete Culture Medium, Phosphate-Buffered Saline (PBS), and Water (H_2O)[a]

	size (nm)			ζ-potential (mV)		
		DDLS (d_h)				
	TEM (d_c)	H_2O	RPMI + HP	H_2O	PBS	RPMI + HP
Citrate-GNS	13.4 ± 2.3	16.8 ± 0.1	48.0 ± 0.5	−34.7 ± 1.0	Aggregated	−9.7 ± 2.1
PEG-GNS	15.7 ± 1.9	26.8 ± 0.3	27.1 ± 0.2	−5.8 ± 1.3	−6.8 ± 0.8	−7.4 ± 1.4
PEG/PVA-GNS	14.6 ± 1.8	23.7 ± 0.8	25.5 ± 1.6	−6.5 ± 0.9	−13.7 ± 0.9	−8.9 ± 1.6
PEG-GNR	length: 57 ± 12 width:15 ± 3	34.8 ± 0.2	33.9 ± 0.3	−13.6 ± 1.5	−3.4 ± 1.7	−9.9 ± 2.9
GNR	n/a	20.7 ± 0.3	n/a	n/a	n/a	n/a

[a] d_c: core diameter. d_h: hydrodynamic diameter. RPMI + HP: complete culture medium consisting of Roswell Park Memorial Institute 1640 with 1% penicillin/streptomycin, 1% L-glutamine, and 10% human plasma.

innate, antigen-independent manner to different stimuli following activation *via* conserved pattern-recognition receptors, *i.e.*, Toll-like receptors (TLRs). This initial innate stimulation critically modulates subsequent activation and differentiation of B cells.[5] Thus, in consideration of the human health impact of exposure to NPs it is imperative to understand how NPs may affect B cells, including their possible cytotoxic profile, as well as their ability to modulate their innate immune function.

The immunotoxicity of NPs has, to date, been studied essentially upon myeloid immune cells such as macrophages and dendritic cells. The phagocytotic nature of these cells leads to engulfment of the NPs, which in turn can promote interference with immune functions.[6] Thus, some types of NPs (*e.g.*, carbon nanotubes, zinc oxide and silica NPs) can cause dysfunctions in cell-intrinsic mechanisms such as autophagy and increases in secretion of pro-inflammatory cytokines, which consequentially may trigger oxidative stress and potentially genotoxicity.[7−9] To minimize the potential toxicity of NPs and to improve their half-life in the body, NP surface functionalization integrated with protective polymer surface coatings are used. Polyethylene glycol (PEG) and poly(vinyl alcohol) (PVA) as well as their copolymer formulation are commonly used as protectors in cosmetic products, food supplements and pharmaceuticals.[10,11] However, use of these polymer coatings for NPs designed for therapeutic applications also has undesired effects: it may lead to the production of antipolymer antibodies, which cause NP opsonization. This then increases clearance of the NPs and therefore affects the efficacy of treatment.[12] To better evaluate the safety of the NPs for the immune system as a whole therefore, it is important to understand distinct effects that NPs may have on different immune subsets. Moreover, direct impact of NPs on B lymphocytes is currently a significant knowledge gap in the field, evidenced by the limited literature on the topic.

Among the variety of nanomaterials available, gold core-based nanoparticles (GNPs) are frequently used as nanomedical tools in therapy, diagnostics and drug delivery. The

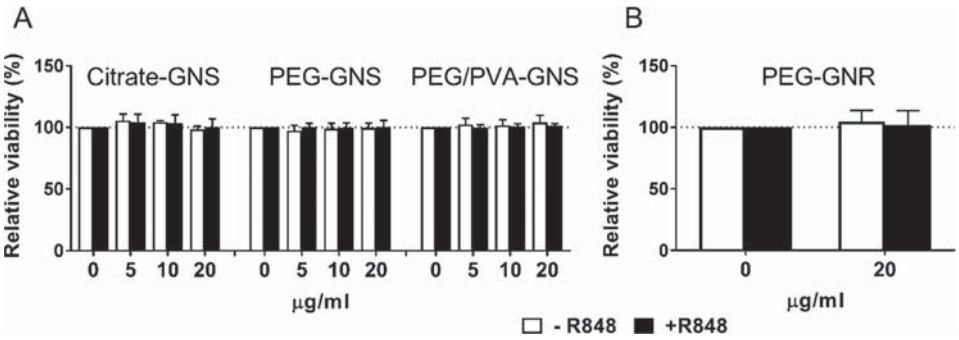

Figure 2. GNPs do not impact upon B lymphocyte viability. Viability of human B lymphocytes was determined by staining cells with Zombie NIR viability dye (1:1000) and measured by flow cytometry after 24 h exposure to GNS (5−20 μg/mL) with different surface functionalizations (A) or to PEG-GNR (20 μg/mL) (B). Cells were incubated with and without the immunostimulant R848 (2 μg/mL). Data are presented relative to control cells without GNP exposure (= 100%). Data represent mean ± SD of three separate experiments on different donors (n = 3). Data were assessed by a two-way ANOVA, followed by Tukey's multiple comparison *posthoc* test. The α value was set at 0.05.

optical properties of GNPs and their high biocompatibility make them highly useful imaging tools, biosensors, and nanocarriers.[13] Furthermore, GNPs efficiently deliver vaccines and immunotherapies to immune cells, achieving effective immune responses with low amounts of cargo.[14,15] In view of the emerging strategies to target B lymphocytes with nanocarriers, and the lack of information about NP immunotoxicity on B cells, we have investigated here the impact of a set of well-characterized GNPs on the phenotype and function of freshly isolated $CD20^+$ human B lymphocytes from peripheral blood.

RESULTS

GNPs with Different Polymer Coatings and Shapes Were Observed To Be Stable in a Biological Environment. To examine the impact of GNPs on B lymphocytes, we selected a panel of GNPs with different functionalizations and shapes that have previously been well characterized. Specifically, these were citrate-stabilized gold nanospheres (Citrate-GNS) and polymer-functionalized gold nanospheres coated either with PEG (PEG-GNS) or a combination of PEG and PVA (PEG/PVA-GNS), as well as PEGylated gold nanorods (PEG-GNR).[16,17] Gold core diameters were measured by transmission electron microscopy (TEM) as 13.4 ± 2.3, 15.7 ± 1.9, and 14.6 ± 1.8 nm for citrate-GNS, PEG-GNS, and PEG/PVA-GNS, respectively. Dimensions of the PEG-GNR were measured at 57 ± 12 nm × 15 ± 3 nm, giving an aspect ratio of 3 ± 0.8 (Figure 1A and Table 1).

UV−vis measurements confirmed the stability in H_2O of all GNPs, as previously described (Figure 1B).[18] Since biological media can affect NP colloidal stability,[19,20] GNPs were incubated for 24 h at 37 °C, 5% CO_2 in complete cell culture media supplemented with 10% human plasma (Roswell Park Memorial Institute 1640 medium + human plasma (RPMI + HP)) or in PBS. A loss in stability was observed for citrate-GNS due to aggregation in culture media, as previously described.[21] Complete aggregation of Citrate-GNS was present in PBS (Figure 1B). In contrast, no signs of increased colloidal instability were detected for either type of polymer-coated GNS or the PEG-GNR.

To further examine their colloidal stability, the hydrodynamic diameter of GNPs in biological media was characterized (Table 1). Negatively charged, nonpolymer coated, citrate-stabilized NPs are known to interact strongly with a protein-rich environment, leading to a change in hydrodynamic diameter due to the formation of a protein corona.[22−24] Indeed, dynamic depolarized light scattering (DDLS) results showed a strong increase in citrate-GNS diameter in RPMI + HP compared to H_2O. For polymer-coated GNPs, the radius did not change in cell culture media, suggesting that a high-density PEG or PEG/PVA coating of the GNPs prevented surface protein adsorption.[25] In addition, PEG-GNR were tested for the efficiency of PEG coverage in relation to cetyltrimethylammonium bromide (CTAB) residues that might still be present from the synthesis. The results shown in Table 1 reveal that PEGylated GNRs presented higher hydrodynamic radii than the as-synthesized GNRs: 34.8 ± 0.2 nm *vs* 20.7 ± 0.3 nm. The surface-grafted PEG chains can acquire either a "brush" or "mushroom" conformation. The latter mainly occurs when the attachment distance of PEG to the surface (D) is larger than the Flory radius (R_F), while the brush conformation is observed when D is smaller than R_F.[26] PEGylated GNRs presented a grafting coverage of 0.22 PEG molecules per nm^2 and D of 2.26 nm, as obtained by a method previously described.[27] This indicated that the PEG layers deposited on the GNRs possessed a brushlike conformation because the R_F for 5000 Da PEG is 4.9 nm. This allowed us to conclude that no potential interference of otherwise toxic CTAB[28] remained on the surface of the GNRs.[29]

The significance of the NP surface charge and the role that it plays in the NP−cell interface is frequently stressed.[30,31] We assessed the effect of the biological environment on the surface charge of GNPs and found that the charge of citrate-GNS considerably changed in RPMI + HP compared to H_2O, most likely due to the surface adsorption of the plasma protein.[32,33] In contrast, polymer-coated GNPs presented a slightly negative charge in both H_2O and RPMI + HP with no major change (Table 1). This confirms that surface charge can vary significantly depending on the GNP surface chemistry; therefore, well-designed polymer functionalization is needed in order to avoid unwanted interactions of GNPs with biological media.

GNPs Do Not Affect B Lymphocyte Viability. The biological impact of GNPs on immune cells varies according to their physicochemical properties. Several groups have shown that characteristics such as size, shape, and polymer coating affect the toxicity of GNPs on macrophages and dendritic cells.[34−36] To assess whether the GNPs described above

impact B lymphocyte viability, total $CD20^+$ human B lymphocytes were freshly isolated from the blood of healthy donors and exposed to increasing concentrations of GNPs. This cell population consists mainly of naive B cells (65−75%) with 20−25% memory B cells.[37] A 24 h exposure time was selected in order to detect early B-cell responses toward GNPs. Then cells were stained with amine-reactive fluorescent viability dye (Zombie NIR) and analyzed by flow cytometry. The polymer-functionalized GNS (PEG and PEG/PVA) as well as citrate-GNS caused no significant cell death at concentrations up to 20 μg/mL (Figure 2A). PEG-GNR, studied at the highest concentration of 20 μg/mL only, also did not impact B cell viability. This latter finding demonstrating that neither the type of polymer coating nor geometry impacts upon B cell viability following GNP exposure (Figure 2B). In addition, phase contrast images did not show decrease in B cell density nor a change in cell morphology upon 24h GNP exposure (Figure S1A).

The small molecule R848 has been reported as an antigen-independent immune activator and stimulator of B lymphocyte proliferation by signaling *via* the receptor TLR7.[38,39] Importantly, B cell viability was not compromised following exposure to GNPs together with the stimulant, irrespective of their shape or functionalization (Figure 2).

Citrate-GNPs Are Taken up by B Lymphocytes, But Not Polymer-Coated GNPs. B lymphocytes are professional antigen-presenting cells, and as such they have the ability to take up pathogens, in particular *via* B cell receptor-mediated endocytosis.[40] To examine whether B lymphocytes could take up GNPs, freshly isolated human B cells were exposed to GNPs for 24 h. The highest GNP concentration tested (20 μg/mL) was considered to be in the sublethal range as it did not cause significant B cell death. Therefore, it was further used in NP-cell association experiments. Macrophages and dendritic cells are professional phagocytotic cells and known to easily take up NPs.[41] Therefore, human monocyte-derived macrophages (MDMs) and monocyte-derived dendritic cells (MDDCs) were also exposed to the previously described GNPs under the same conditions as the B cell experiments. MDMs and MDDCs served as a control for GNP-B cell interaction as well as for comparison of GNP-B cell association across different antigen-presenting cell (APC) types.

The cells and the GNP uptake were first visualized by dark field hyperspectral imaging (DF-HSI) coupled with fluorescent detection. For citrate-GNS, which were noted to readily aggregate in biological media, clusters of NPs were clearly visible on the surface of B cells (Figure 3A). The particles were also detectable within the B cells themselves (insert Figure 3A). Citrate-GNS were further observed to be internalized by MDMs and MDDCs, as expected for these highly phagocytotic cell types (Figure 3A and Figure S1B and S1C). In contrast to citrate-stabilized GNS, no interaction (either internalization or cell surface association) of polymer-coated GNS with B lymphocytes was detected by DF-HSI. Similarly, PEG-GNR did not show any association with B cells (Figure S3). In MDMs, only a few intracellular aggregates of PEG-GNS and PEG/PVA-GNS were detected by DF-HSI (Figure 3A).

A subsequent approach to determine NP internalization by mammalian cells is through changes in light scattering detected by flow cytometry. This was previously reported by Zucker *et al.*,[42] who demonstrated that the internalization of TiO_2 NPs increased side scatter (SSC) and decreased forward scatter (FSC) by epithelial cells. An increase in SSC was observed for

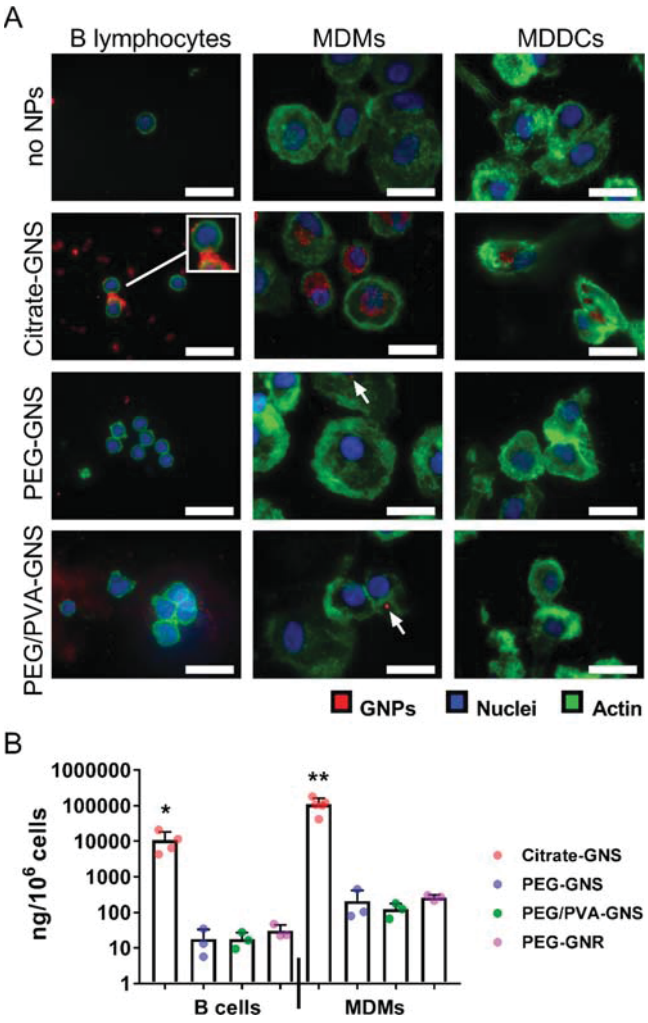

Figure 3. Polymer-coated GNPs cause limited B lymphocyte uptake. (A) Dark field hyperspectral images of B cells and other antigen-presenting cells exposed to GNS at 20 μg/mL for 24 h. Scale bars: 5 μm. The white arrows indicate intracellular GNS. (B) Quantification by ICP-MS of gold ion content in B lymphocytes and MDMs exposed to GNPs at 20 μg/mL for 24 h. Each dot represents one biological sample. Bars represent the mean ± SD of three to four biological replicates; *$p < 0.05$, **$p < 0.01$. Data were evaluated by a one-way ANOVA, followed by Tukey's multiple comparison *posthoc* test.

B cells exposed to citrate-GNS but not to polymer-coated GNS (Figure S4). In contrast, in MDMs and MDDCs, an increase in side scatter was observed for polymer-coated GNS. Overall, these results supported the observations collected from the DF-HSI images.

To quantify the uptake of GNPs with human B cells and to compare this to the association by other APCs, we measured the gold content within B cells and MDMs after exposure to 20 μg/mL of GNPs by using inductively coupled plasma mass spectroscopy (ICP-MS). This technique allows precise quantification of the gold ion content in biological samples.[43] The uptake of citrate-GNS by B cells was confirmed, with approximately 10 μg of gold measured per 10^6 cells (calculated by dividing measured GNP mass per total cell count and multiplying by 10^6) (Figure 3B). This corresponds to approximately 1% GNP-B cell association as a function of measured GNP mass per total exposed GNP mass. In contrast,

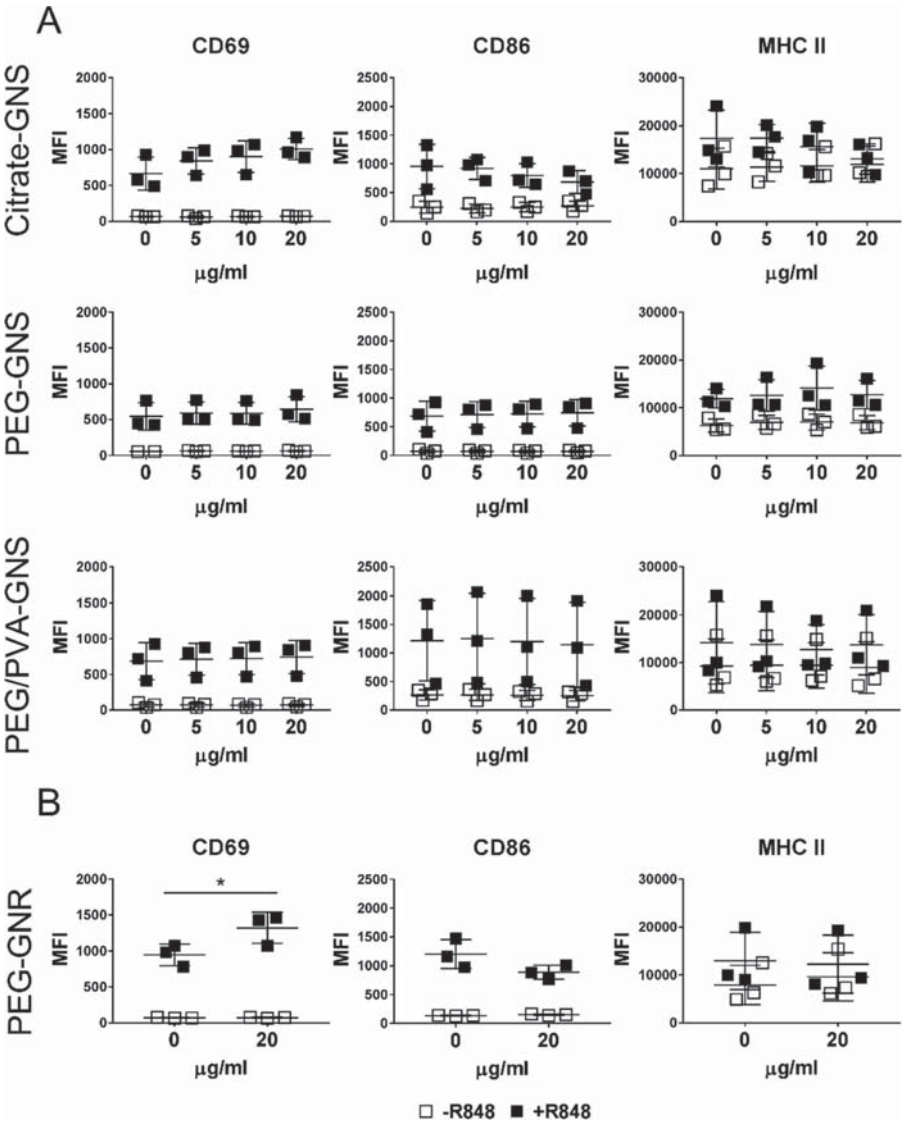

Figure 4. B lymphocyte activation. Surface activation markers on B lymphocytes (CD69, CD86 and MHC-II) measured by flow cytometry after 24 h exposure of B cells to GNS (5−20 μg/mL) with different surface functionalization (A) or to PEG-GNR (20 μg/mL) (B). B cells were incubated with or without the immunostimulant R848 (2 μg/mL). Each point represents one donor (n = 3). Error bars: mean ± SD; *p < 0.05. Data were evaluated by a two-way ANOVA, followed by Tukey's multiple comparison *posthoc* test. The α value was set at 0.05.

polymer-coated GNPs were detected at very low levels in B lymphocytes, confirming the findings obtained by DF-HSI. In comparison to B cells, MDMs internalized polymer-coated GNPs approximately 10 times more efficiently. Similar to B cells, citrate-GNS associated with MDMs with high efficiency compared to the polymer-coated GNS (Figure 3B).

Here, we demonstrate using DF-HSI that primary human B lymphocytes can internalize aggregated citrate-GNPs. This is in accordance with a previous report in a mouse B cell line of the uptake of citrate GNPs aggregates, visualized in the endosomal compartments.[44] Clearly, as shown in the present study, PEG-containing polymer coating prevents the uptake of the GNP both in B cells and in myeloid cells such as macrophages and dendritic cells. This agrees with previous results in dendritic cells, where GNPs coated with the combination of PEG/PVA had a significantly lower uptake than with PVA coating alone, presumably due to the shielding role of PEG.[16] Our current results suggest that shape does not have a significant effect upon the uptake by either B cells or macrophages and dendritic cells. Nevertheless, the exact mechanisms and possible surface receptors involved in the GNP uptake by B lymphocytes across different physiochemical properties of GNPs remain unknown.

GNPs Do Not Impair B Lymphocyte Activation. Since gold-based nanoparticles have been shown in some instances to stimulate B cell lines,[45] we investigated whether the GNPs used in this study could lead to antigen-independent activation of primary human B cells. The immune cell activation markers CD69, CD86, and MHC II were assessed on B cells by flow cytometry after exposure of the cells to GNPs. The TLR7 ligand R848 was used as positive control for antigen-independent B-cell activation.[46] In the absence of R848, expression of activation markers was not increased after exposure to any of the tested GNS at concentrations up to 20 μg/mL for 24 h (Figure 4A). Upon R848 stimulation, B cells showed upregulation of all three activation markers, as expected. Importantly, exposure to GNS did not impair the pharmacological activation of B cells by R848. Similar results

were obtained for PEG-GNR at 20 μg/mL, which neither activated B cells nor inhibited their stimulation by R848 (Figure 4B). The activation status of MDMs and MDDCs exposed to GNS was also assessed: the nanospheres did not activate these cells nor did they impair their stimulation by R848 (Figure S6). Thus, the GNPs used in this study did not stimulate human B cells, and they did not interfere with their drug-induced activation.

Pro-inflammatory Responses Are Not Enhanced by GNPs. Nanoparticles have been shown to induce the production of pro-inflammatory mediators in immune cells.[47] In particular, nanoparticles have been noted as being able to trigger activation of the inflammasome complex, which causes the secretion of pro-inflammatory cytokines such as I-1β.[48] Since inflammation can result in severe side effects in patients, it is essential to test the pro-inflammatory potential of NPs destined for biomedical applications early in their development process. To assess whether GNPs induced the production of pro-inflammatory mediators in B cells, we measured the secretion of the pro-inflammatory cytokines IL-6 and IL-1β by B cells after a 24 h incubation with GNPs, with or without R848. The levels of cytokines were determined by ELISA in the cell culture supernatant. IL-6 and IL-1β secretion was not induced by GNS at concentrations up to 20 μg/mL, regardless of their functionalization, nor by PEG-GNR (Figure 5A). R848 stimulation induced production of both IL-6 and IL-1β by B cells, as expected for a TLR7 agonist, but this cytokine production was not affected by polymer-coated GNS. Interestingly, PEG-GNR at 20 μg/mL caused a significant drop in IL-6 concentration from otherwise increased IL-6 levels of B cells induced by R848 (Figure 5B). Similarly, citrate-GNS caused suppression of IL-6 production in R848-activated cells in a concentration-dependent fashion, although the decrease was not statistically significant due to high variation between the cells from the different donors.

In order to further compare the effect of GNPs across APCs, pro-inflammatory cytokines of MDMs and MDDCs were measured after exposure to all types of GNS at the highest concentration only (20 μg/mL). Similarly to B cells, GNS did not induce cytokine release in the absence of R848. Interestingly, citrate-GNS did not interfere with efficiency of the R848-induced cytokine release by MDMs and MDDCs, in contrast to the observations for activated B lymphocytes (Figure S7).

The potential interference of GNPs, which possess light-absorbing properties, with optical-based assays such as ELISA must be considered. To exclude such an interference, we carefully assessed the potential background caused by GNPs alone in the optical signal of the plate reader and found that all GNPs, even at the highest concentration of 20 μg/mL, were below the detection level of the ELISA (data not shown). Further, we controlled the possible absorbance of cytokines onto the surface of the GNPs, which could impact upon the reliable reading of cytokine concentrations *via* this method. We detected no effect of the GNPs on cytokine concentrations in this cell-free assay (Figure S8).

DISCUSSION

The interactions of GNPs with B lymphocytes are important for biomedical applications, especially in view of the selective targeting of B lymphocytes by NPs. Although B lymphocytes are generally not considered professional phagocytic cells, they are capable of, in theory, actively taking up large particulate

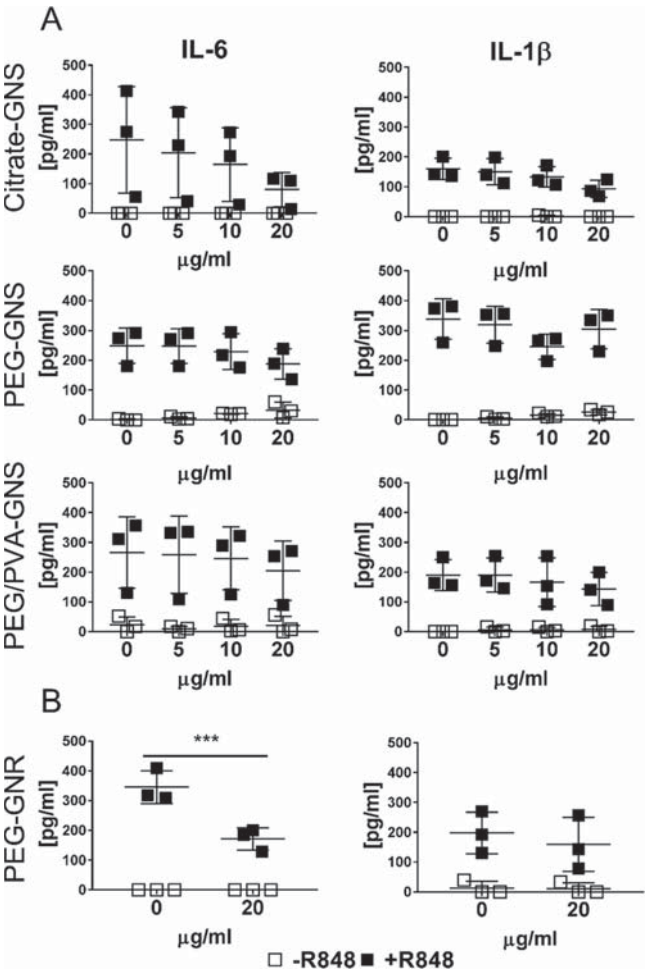

Figure 5. B lymphocyte pro-inflammatory response. Release of pro-inflammatory cytokines after 24 h exposure of B cells to GNS (5−20 μg/mL) with different surface functionalization (A) or to PEG-GNR (20 μg/mL) (B). B cells were incubated with or without the immunostimulant R848 (2 μg/mL). Each point represents one donor (n = 3). Error bars: mean ± SD; ***p < 0.001. Data were evaluated by a two-way ANOVA, followed by Tukey's multiple comparison *posthoc* test. The α value was set at 0.05.

material through B-cell and complement receptors.[49] Our results confirmed that GNPs which have a polymer-protected surface trigger very low uptake by primary human B lymphocytes. In contrast, uncoated GNPs, which were opsonized by plasma proteins, were highly taken up even by naive B cells. This heightened interaction may be due, in part, to the formation of NP aggregates in the cell culture medium, which could trigger stronger internalization by the B cells compared to well-dispersed polymer-coated NPs.[50] It has recently been shown that NP-bound antigens can be efficiently taken up by antigen-specific B lymphocytes, which then act as APCs to stimulate CD4 T cell responses.[51] Taken together, polymer-coated GNPs loaded with antigen may selectively target only those B lymphocytes recognizing their cognate antigen, thus enhancing selectivity of novel vaccine strategies.

Cytotoxicity of GNPs, which depends on size, shape, dose, coating, and surface characteristics, is a major concern. Our results show that the formulations of GNPs used in this study, including uncoated GNS and rod-shaped GNPs, do not cause significant B cell cytotoxicity after 24 h exposure *in vitro*. These results give us valuable information for the further biomedical

development of safe GNPs, particularly those that are foreseen to come in direct contact with the immune system. In addition, gold nanomaterials have immunomodulatory properties and are able to induce activation in immune cells.[52] One of the reasons is the insufficient GNP polymer surface coverage, which initiates binding and deformation of proteins that can then act as immunostimulants.[53,54] Our data provide evidence that GNPs that are well-protected by polymers do not activate B lymphocytes, nor do they interfere with the action of an immunostimulatory drug (R848).

Interestingly, we show that uncoated GNS, which aggregate in biological media, and rod-shaped GNPs impaired IL-6 cytokine production in TLR7-stimulated B lymphocytes. This suggests that the particle shape controls interference with early, antigen-independent activation events in B lymphocytes. However, further studies are needed to clarify possible mechanisms behind this impairment.

CONCLUSION

The safety of NPs and their consequences on the immune system are of crucial importance. Indeed, as stressed by FDA draft guidelines on nanomaterials for the industry, characterization of the nanomaterial should be carefully assessed.[55] The defined physicochemical characteristics of the NPs should be taken into consideration to cross-relate them for their stability in a biological environment and to determine the exact mechanisms of cell type-specific biological responses. Therefore, to evaluate the adequacy of GNP use in clinical studies, the impact of GNPs on the immune system (*e.g.,* immunogenicity and immunotoxicity) is an important aspect that needs to be further investigated and specified. With our study, we have gained insight as to the impact of GNPs on B lymphocytes and showed that the absence of polymer coating and GNP shape are important factors that lead to different outcomes in GNP-B cell association and B cell efficiency of the cytokine release, which should be considered for future development of GNP for biomedical use.

METHODS

Chemicals and Reagents. All of the chemicals were used without further purification. All chemicals and reagents purchased from Sigma-Aldrich (Switzerland) were used as received, unless otherwise stated.

GNP Synthesis. Methoxypolyethylene glycol thiol (mPEG-SH; 5 kDa) was purchased from Creative PEGWorks. Poly(vinyl alcohol) (PVA, Mowiol 3-85, 14 kDa) was purchased from Omy AG. All glassware was cleaned with *aqua regia* and extensively rinsed with water prior to use. Milli-Q grade water was used in all preparations.

Citrate-stabilized gold nanoparticles (GNPs) 15 nm in diameter were synthesized as previously described by Turkevich *et al.*[56] Briefly, the aqueous solution of tetrachloroauric acid ($HAuCl_4{\cdot}3H_2O$; 500 mL, 0.5 mM) was heated to 100 °C and allowed to boil for 10 min, which was followed by rapid addition of 25 mL of 34 mM sodium citrate previously heated to 60 °C. Within 20 min, the color of the solution changed to red, indicating the formation of GNPs. After cooling to the room temperature, NPs were kept in the glass container, in the dark, and at a temperature of 4 °C.

Preparation of PEG-GNS. An aqueous solution of mPEG-SH (3.4 mg/mL, 2.5 mL), equivalent to 10 PEG nm^{-2}, was sonicated for 30 min and was subsequently mixed with 50 mL of citrate-coated GNS suspension. The mixture was allowed to react at room temperature for 24 h. To remove any excess polymer, the PEGylated GNS were centrifuged at 10000*g* for 1 h and redispersed in water.

Preparation of PEG/PVA-GNS. Separately, an aqueous solution containing 6 mg of poly(vinyl alcohol) (PVA) and 6 mg of mPEG-SH was prepared and sonicated for 20 min. Then the polymer solution was added dropwise at room temperature under shaking to GNS suspension (20 mL). The mixture was left overnight under dark conditions. The final GNS-PEG/PVA suspension was then centrifuged (10000*g*, 1 h) to remove excess polymer and redispersed in water.

Synthesis of GNRs. GNRs were prepared by the seed-mediated growth method.[57] The Au seeds were synthesized by mixing a hexadecyltrimethylammonium bromide (CTAB) solution (0.1 M, 4.7 mL) with $HAuCl_4{\cdot}3H_2O$ (50 mM, 0.025 mL) at 28 °C for 5 min. To this solution was added fresh sodium borohydride ($NaBH_4$) aqueous solution (10 mM, 0.3 mL) under vigorous stirring for 2 min. The mixture immediately turned light brown, indicating the formation of seed particles. The seed dispersion was aged for 1 h at 28 °C before use. Separately, a gold growth solution was prepared by adding $HAuCl_4{\cdot}3H_2O$ solution (50 mM, 2.23 mL) to CTAB (0.1 M, 200 mL) and mixed by inversion. Silver nitrate ($AgNO_3$) was then added (10 mM, 2.6 mL), followed by HCl (1 M, 3.84 mL), and mixed again by inversion. Next, L-ascorbic acid was added (0.1 M, 1.6 mL), and the solution was mixed vigorously until the solution turned colorless. Finally, the Au seeds (960 μL) were added to the growth solution and followed by brief inversion mixing. The resulting suspension was left overnight at 28 °C for the GNR formation. GNRs then underwent further manipulation in order to have a polymer coating.

Preparation of PEG-GNR by a Two-Step Method. PEGylated GNRs were prepared as previously described by Kinnear *et al.*[29] Briefly, the GNRs (10 mL, [Au] = 0.15 mM) were purified twice by centrifugation (8000*g* for 50 min) leading to a residual [CTAB] = 0.1 mM. Under shaking, a solution of mPEG-SH was added (10 mg/mL, 50.5 μL), equivalent to 10 PEG nm^{-2}, and mixed over 24 h. The partially PEGylated GNRs were then centrifuged at 8000*g* for 50 min and redispersed in ethanol (90% v/v ethanol, 9.5 mL). To this, an ethanolic solution of mPEG-SH (1 mg/mL in 90% v/v ethanol, 505 μL) was added under shaking and gently mixed over 24 h. Finally, completely PEGylated GNRs were centrifuged three times at 8000*g* for 50 min to remove unreacted PEG and displaced CTAB with redispersion in water.

GNP Characterization. *Transmission Electron Microscopy.* GNP diameter was assessed through TEM, operating at 120 kV (FEI Technai Spirit microscope, USA) and equipped with a Veleta CDD camera (Olympus, Japan). In order to avoid drying-related artifacts of drop-casting, Citrate-GNS and PEG-GNR TEM samples were prepared as previously described.[58] Briefly, samples were suspended in a 1:1 ratio in the corresponding concentration of bovine serum albumin (BSA, Sigma-Aldrich, USA) solution and left at 4 °C overnight. Polymer-coated GNS samples were prepared without BSA incubation in order to obtain more dense images of these type of NPs. A total of 5 μL of BSA-GNP (citrate-GNS, PEG-GNR) or GNP sample in H_2O alone (PEG-GNS, PEG/PVA-GNS) was drop-casted on mash copper grids at a final GNP concentration 20 μg/mL and left to dry at room temperature. GNP size was subsequently calculated using ImageJ software at the following NP count: citrate-GNS: n = 132; PEG-GNS: n = 103, PEG/PVA-GNS: n = 149, PEG-GNR: n = 220. Endotoxin levels of GNPs were determined by a Pierce LAL Chromogenic Endotoxin Quantitation Kit (ThermoFisher, Switzerland), following the manufacturer's guidelines (Figure S9).

UV–vis. UV–vis spectra of GNPs were obtained using a JASCO V-670 spectrophotometer. The colloidal stability was tested by incubation of GNPs in H_2O, 10 mM PBS, and culture medium (RPMI 1640 (Roswell Park Memorial Institute) with 10% human plasma, 1% PenStrep and 1% L-glutamine) for 24 h at 37 °C, 5% CO_2. All GNPs were diluted to a concentration of 0.01 mg/mL in each solution.

Dynamic Depolarized Light Scattering. Citrate-GNS, PEG-GNS, PEG/PVA-GNS (all at 5 μg/mL), and PEG-GNR (20 μg/mL) were incubated in water or culture medium (RPMI with 10% human plasma, 1% PenStrep, and 1% L-glutamine) at 37 °C for 24 h. Then DDLS measurements were performed at constant temperature (21 °C) at a scattering angle of 30° using a commercial goniometer instrument (3D LS spectrometer, LS Instruments AG, Switzerland).

To estimate the number-averaged hydrodynamic radii, the DDLS spectra were analyzed by the approach presented elsewhere.[59]

ζ-potential. GNP charge was acquired with a phase-amplitude light-scattering analyzer (PALS) (Brookhaven ZetaPALS). GNPs were measured at 0.05 mg/mL at rt in H_2O (pH 7), PBS (pH 7) and culture media (pH 7), where PBS and media were prediluted in H_2O to 1:10. Measurements for each sample were obtained using the Smoluchowski model[60] with 10 cycles of electrophoretic mobility (EPM) and 10 repetitions to gain mean and standard deviation data. All incubations of GNPs in the cell-free biological media were solely performed for GNP characterization purposes.

Immune Cell Cultures. *Human B Lymphocytes.* Buffy coats from healthy donors (BlutZentrum, Bern, Switzerland) were separated by gradient density (Lymphoprep, Stemcell Technologies, Canada) followed by specific B lymphocyte magnetic bead isolation using anti-CD20 MicroBeads (Miltenyi Biotec, Germany). Fc receptor blocking reagent (Miltenyi Biotec) was added according to the manufacturer's instructions. A purity of >96% $CD20^+$ cells was obtained throughout the experiments (Figure S5). B lymphocytes were cultured in six-well plates (0.25×10^6 cells/mL) at 37 °C, 5% CO_2 in RPMI 1640, supplemented with 10% autologous human plasma from each donor, 1% PenStrep (ThermoFisher Scientific, USA, No. 15140122) and 1% L-glutamine (ThermoFisher, Scientific, USA, No. 25030081). The seeding concentration was chosen based on the median B lymphocyte number typically found in healthy human peripheral blood.[61]

Monocyte Subculture. Monocytes were isolated from buffy coats with anti-CD14 MicroBeads (Miltenyi Biotec) and cultured in six-well plates (10^6 cells/ml).[62] Fc receptor blocking reagent (Miltenyi Biotec) was added in the purification protocol. In order to differentiate monocytes from macrophages (monocyte-derived macrophages, MDM) or dendritic cells (monocyte-derived dendritic cells, MDDC), 10 ng/mL macrophage colony-stimulating factor (M-CSF) or 10 ng/mL granulocyte-macrophage colony-stimulating factor (GM-CSF) and 10 ng/mL IL-4 were added into the culture, respectively, and incubated for 6 days at 37 °C, 5%CO_2. All cell types were cultured at 37 °C, 5% CO_2 in RPMI 1640, supplemented with 10% autologous human plasma from each donor, 1% PenStrep (ThermoFisher Scientific, USA, No. 15140122) and 1% L-glutamine (ThermoFisher, Scientific, USA, No. 25030081).

Exposure to GNPs and Stimulants. *B Lymphocytes.* Cells were exposed to all GNS directly after purification for 24 h at concentrations from 5 to 20 μg/mL and to PEG-GNR at 20 μg/mL.

MDMs/MDDCs. Cells were exposed to all GNS on day 6 of culture at 20 μg/mL for 24 h. R848 (Enzo, USA) at 2 μg/mL was used for B lymphocyte/MDM/MDDC and LPS control at 100 ng/mL (Sigma-Aldrich, Switzerland) was used for MDM/MDDC stimulation. The working concentrations of these immunostimulants was selected in order to induce robust activation in all donor samples.

GNP-Cell Association Assessment. *Light Microscopy.* Phase contrast images were captured at a magnification ×40 using an inverted light microscope (Motic AE2000, Germany) after 24 h NP exposure (Figure S1).

Enhanced Dark-Field Optical Microscopy with High-Resolution Hyperspectral Imaging. Cells exposed to GNPs were fixed with 4% paraformaldehyde (PFA), permeabilized with 0.01% TritonX-100 (Sigma-Aldrich, Switzerland) in PBS and stained with rhodamine-phalloidin, diluted 1:40 in PBS and 4′,6-diamidino-2-phenylindole (DAPI) using dilution 1:100 in PBS. Samples were imaged with high signal-to-noise ratio dark field hyperspectral imaging that uses oblique angle lighting (CytoViva, Alburn, AL). The system is coupled with an Olympus BX-51 microscope outfitted with a fluorescence light source (X-Cite series 120), halogen light source (Dolan-Jenner DC-950), UPL Fluorite 100× objective, and SPECIM V10E imaging spectrograph with a PCO pixelfly detector (Kelhelm, Germany). All data acquisition was preformed using the same exposure time and magnification (100× oil immersion). Images from both dark field and fluorescent imaging were recorded using a 3D Exi blue camera (QImaging, Surry, Canada) and ENVI 4.8 software. Images obtained from both sources were overlaid using ImageJ software. Hyperspectral images were recorded using the same system and software but in spectral mode, using above-mentioned detector. Due to the strong scattering of light, gold nanoparticles appear as the brightest signal on the image. Linear enhancement was used to obtain the best contrast of the object against the image background. This type of enhancement shows the full intensity range, from lowest to highest, without clipping.

ICP-MS Chemicals. Acids (HNO_3, HCl) were of PlasmaPure grade from SCP Science (Courtaboeuf, France). Ultrapure deionized water was provided by an Integral 3 Advantage A10 purification system (Merck-Millipore, Schaffhausen, Switzerland). The ICP-MS certified tuning solution consisted of 1 μg/L each of Li, Mg, Y, Ce, Tl and Co in a matrix of 2% HNO_3 was from SCP Science (catalog no. 701-021-194 5185-5959, batch no. S171122014). The gold certified standard solution (1000 ppm in 5% HCl) was purchased from Sigma-Aldrich (catalog no. 38168-100 ML, batch no. BCBT4405).

Sample Preparation. B lymphocytes and MDMs were cultured and exposed to GNPs as described above. After 24 h, cells of one to three plates were pooled (cells in 18−54 mL), washed two times in 1× PBS (500*g*, 4 °C, 5 min), and counted (total cell number of the sample). After final centrifugation, supernatant was discarded and cell pellets were stored at −20 °C until further analysis. Cell pellets were resuspended in 4.5 mL of ultrapure Milli-Q water, with addition of 0.5 mL of concentrated *aqua regia* (HNO_3/HCl, 1:3), and digested by heating block for 1 h at 80 °C (EasyDigest, Analab, France). Then digested cell pellets were diluted in 10% (v/v) aqueous *aqua regia* (10% AR) to be within the calibration range of the ICP-MS method. Final quantification of GNP-cell association was calculated as ng/10^6 cells by dividing measured GNP mass per total cell number of each sample (cell count prior obtaining the cell pellet) and multiplication by 10^6.

Instrumentation. The Agilent 7700x ICP-MS system (Agilent Technologies, Basel, Switzerland) was equipped with a Micromist nebulizer and a Scott-type spray chamber. The ICP-MS parameters were tuned with a certified solution to obtain the best sensitivity, resolution, and lower RSD on ^{7}Li, ^{89}Y, and ^{205}Tl and also the lower oxide (156/140, CeO/Ce) and doubly charged (70/140, Ce^{2+}/Ce) ratios. The ICP-MS parameters were optimized for the three collision cell modes (Table S1).

ICP-MS Method. Gold (^{197}Au) was quantified (n = 3) by ICP-MS with and without the use of a collision cell (CC), respectively termed [He] or [HEHe] and [no gas] mode. The two collision cell modes, [He] and [HEHe], with helium gas at two flow rates, 4.3 mL/min and 10 mL/min, respectively, allow removal or reduction of the potential spectral interferences. The ICP-MS calibration curve consisted of one blank (10% AR) and eight ^{197}Au concentration levels (0.1, 0.5, 1, 5, 10, 15, 20, 25 ppb in 10% AR). The linear regression correlation coefficients (R) were equal to 0.9997, 0.9995, and 0.9995 for ^{197}Au measured in [no gas], [He], and [HEHe] modes, respectively (Figure S2), which was in agreement with the FDA guidelines ($R \geq 0.998$).[63] Evaluation of the ICP-MS method accuracy and precision was also evaluated. The results fulfill the precision (RSD ≤ 15%) and accuracy (100% ± 15%) criteria.[43]

Flow Cytometry: Cell Viability and Immune Cell Status. Cells were stained for 15 min at room temperature with a Zombie NIR Fixable Viability Kit (BioLegend, USA) and washed with FACS buffer (1% BSA, 0.5% sodium azide (Sigma-Aldrich, Switzerland) in PBS). Cells were then stained for 30 min with the following antibodies at 1:100 (unless stated otherwise). *B cells:* antihuman CD20-FITC (B cell-specific marker, BD Biosciences, USA), antihuman CD69-Pacific Blue (BioLegend, USA), CD86-PE-Cy5 (BioLegend, USA), and HLA-DR-PE-CF594 (at 1:300, BD Biosciences, USA). *MDMs:* CD14-FITC (monocyte/macrophage-specific marker, BioLegend, USA), CD69-PacificBlue (BioLegend, USA), CD86-PE-Cy5 (BioLegend, USA), HLA-DR-PE-CF594 (at 1:300, BD Biosciences, USA). *MDDCs*: CD1c-PacificBlue (dendritic cell-specific marker, BioLegend, USA), CD80-FITC, CD86-PE-Cy5 (BioLegend, USA), HLA-DR-PE-CF594 (at 1:300, BD Biosciences, USA). Cells were then washed and resuspended in 0.5 mL of FACS buffer for flow cytometer analysis (BD LSR Fortessa, Switzerland). Three

independent experiments were performed for each cell type, and each sample was set up to capture up to 30000 events. Gating strategies for all cell types are shown and explained in the Supporting Information (Figure S5). All flow cytometry data were analyzed with FlowJo software (Version 10, Tree Star, USA).

Pro-inflammatory Response. After 24 h exposure of immune cells to GNPs, culture supernatants were collected and measured for concentrations of interleukin (IL)-6, IL-1β, and tumor necrosis factor (TNF)-α by ELISA. The assay was performed according to the manufacturer's instructions (Human IL-6 DuoSet ELISA, Human IL-1β/IL-1F2 DuoSet ELISA, and Human TNF-α DuoSet ELISA, all from R&D, USA). The experiment for each analyte was conducted three times in duplicate (n = 3).

To ensure that GNPs did not interfere with the spectrophotometric analysis, an interference test were performed for the IL-6 ELISA kit: GNPs (20 μg/mL) alone were incubated in complete culture media for 24 h at 37 °C, 5% CO_2. Prior to the ELISA being conducted, GNP samples were incubated with a IL-6 standard (0−600 pg/mL) for 1 h at rt. Optical density for all the ELISA samples was measured at 450/570 nm using a microplate reader (Benchmark Microplate reader, BioRad, Cressier, Switzerland). The test experiments were performed once in triplicate (Figure S8).

Data and Statistical Analysis. Results are presented as a mean of three separate experiments (three different donors (n = 3)) ± standard deviation (SD). Data were considered normally distributed and thus were evaluated using a nonparametric two-way analysis of variance (ANOVA) or one-way ANOVA. Subsequent analysis occurred in terms of a Tukey's multiple comparison *posthoc* test (GraphPad Prism 7 software, USA). Data was considered significant when $*p < 0.05$, $**p < 0.01$, and $***p < 0.001$.

ASSOCIATED CONTENT

Supporting Information

The Supporting Information is available free of charge on the ACS Publications website at DOI: 10.1021/acsnano.9b01492.

SEM method, light microscopy images of APCs, details about optimization of the ICP-MS method, additional DF-HSI image, GNP-cell association and FSC/SSC signal, cell purity and gating strategy, MDM and MDDC activation, MDM and MDDC pro-inflammatory response, and GNP interference test (PDF)

AUTHOR INFORMATION

Corresponding Authors

*E-mail: m.j.d.clift@swansea.ac.uk.
*E-mail: carole.bourquin@unige.ch.

ORCID

Sandra Hočevar: 0000-0002-9770-8229
Ines Mottas: 0000-0002-9027-7577
Alke Petri-Fink: 0000-0003-3952-7849
Carole Bourquin: 0000-0003-3862-4583
Martin James David Clift: 0000-0001-6133-3368

Present Addresses

#(A.M.) Empa, 9014 St. Gallen, Switzerland.
⊗(L.R.-L.) Nano4Environment Unit, Water Quality Group, INL - International Iberian Nanotechnology Laboratory, 4715-330 Braga, Portugal.

Author Contributions

▽C.B. and M.J.D.C. contributed equally.

Notes

The authors declare no competing financial interest.

ACKNOWLEDGMENTS

The authors acknowledge the support by the Swiss National Science Foundation (SNSF) through the National Centre of Competence in Research "Bio-Inspired Nanomaterials" and project nos. 156871, 156372, and 182317, the Adolphe Merkle foundation (Fribourg, Switzerland), and the MZ 2.0 mass spectrometry core facility (University of Geneva) for the ICP-MS method development and sample measurements.

REFERENCES

(1) Lebien, T. W.; Tedder, T. F. ASH 50th Anniversary Review B Lymphocytes : How They Develop and Function. *Blood* **2008**, *112*, 1570−1580.
(2) Pardi, N.; Hogan, M. J.; Naradikian, M. S.; Parkhouse, K.; Cain, D. W.; Jones, L.; Moody, M. A.; Verkerke, H. P.; Myles, A.; Willis, E.; LaBranche, C. C.; Montefiori, D. C.; Lobby, J. L.; Saunders, K. O.; Liao, H.-X.; Korber, B. T.; Sutherland, L. L.; Scearce, R. M.; Hraber, P. T.; et al. Nucleoside-Modified mRNA Vaccines Induce Potent T Follicular Helper and Germinal Center B Cell Responses. *J. Exp. Med.* **2018**, *215*, 1571−1588.
(3) Fenton, O. S.; Kauffman, K. J.; Kaczmarek, J. C.; McClellan, R. L.; Jhunjhunwala, S.; Tibbitt, M. W.; Zeng, M. D.; Appel, E. A.; Dorkin, J. R.; Mir, F. F.; Yang, J. H.; Oberli, M. A.; Heartlein, M. W.; DeRosa, F.; Langer, R.; Anderson, D. G. Synthesis and Biological Evaluation of Ionizable Lipid Materials for the *In Vivo* Delivery of Messenger RNA to B Lymphocytes. *Adv. Mater.* **2017**, *29*, 1−7.
(4) Shen, X.; Pasha, M. A.; Hidde, K.; Khan, A.; Liang, M.; Guan, W.; Ding, Y.; Haczku, A.; Yang, Q. Group 2 Innate Lymphoid Cells Promote Airway Hyperresponsiveness through Production of VEGFA. *J. Allergy Clin. Immunol.* **2018**, *141*, 1929−1931.e4.
(5) Hua, Z.; Hou, B. TLR Signaling in B-Cell Development and Activation. *Cell. Mol. Immunol.* **2013**, *10*, 103−106.
(6) Boraschi, D.; Italiani, P.; Palomba, R.; Decuzzi, P.; Duschl, A.; Fadeel, B.; Moghimi, S. M. Nanoparticles and Innate Immunity: New Perspectives on Host Defence. *Semin. Immunol.* **2017**, *34*, 33−51.
(7) Kojima, S.; Negishi, Y.; Tsukimoto, M.; Takenouchi, T.; Kitani, H.; Takeda, K. Purinergic Signaling *via* $P2X_7$ Receptor Mediates IL-1β Production in Kupffer Cells Exposed to Silica Nanoparticle. *Toxicology* **2014**, *321*, 13−20.
(8) Turabekova, M.; Rasulev, B.; Theodore, M.; Jackman, J.; Leszczynska, D.; Leszczynski, J. Immunotoxicity of Nanoparticles: A Computational Study Suggests That CNTs and C_{60} Fullerenes Might Be Recognized as Pathogens by Toll-like Receptors. *Nanoscale* **2014**, *6*, 3488−3495.
(9) Xi, C.; Zhou, J.; Du, S.; Peng, S. Autophagy Upregulation Promotes Macrophages to Escape Mesoporous Silica Nanoparticle (MSN)-Induced NF-KB-Dependent Inflammation. *Inflammation Res.* **2016**, *65*, 325−341.
(10) Debotton, N.; Dahan, A. Applications of Polymers as Pharmaceutical Excipients in Solid Oral Dosage Forms. *Med. Res. Rev.* **2017**, *37*, 52−97.
(11) European Food Safety Authority (EFSA).. Scientific Opinion on the Safety of Polyvinyl Alcohol-Polyethylene Glycol-Graft-Co-Polymer as a Food Additive. *EFSA J.* **2013**, *11*, 3303.
(12) Lubich, C.; Allacher, P.; de la Rosa, M.; Bauer, A.; Prenninger, T.; Horling, F. M.; Siekmann, J.; Oldenburg, J.; Scheiflinger, F.; Reipert, B. M. The Mystery of Antibodies Against Polyethylene Glycol (PEG) - What Do We Know? *Pharm. Res.* **2016**, *33*, 2239−2249.
(13) Dykman, L.; Khlebtsov, N. Gold Nanoparticles in Biomedical Applications: Recent Advances and Perspectives. *Chem. Soc. Rev.* **2012**, *41*, 2256−2282.
(14) Climent, N.; García, I.; Marradi, M.; Chiodo, F.; Miralles, L.; José Maleno, M.; María Gatell, J.; García, F.; Penadés, S.; Plana, M. Loading Dendritic Cells with Gold Nanoparticles (GNPs) Bearing HIV- Peptides and Mannosides Enhance HIV-Specific T Cell Responses. *Nanomedicine* **2018**, *14*, 339−351.

(15) Assis, N. R. G.; Caires, A. J.; Figueiredo, B. C.; Morais, S. B.; Mambelli, F. S.; Marinho, F. V.; Ladeira, L. O.; Oliveira, S. C. The Use of Gold Nanorods as a New Vaccine Platform against Schistosomiasis. *J. Controlled Release* **2018**, *275*, 40−52.
(16) Rodriguez-Lorenzo, L.; Fytianos, K.; Blank, F.; Von Garnier, C.; Rothen-Rutishauser, B.; Petri-Fink, A. Fluorescence-Encoded Gold Nanoparticles: Library Design and Modulation of Cellular Uptake into Dendritic Cells. *Small* **2014**, *10*, 1341−1350.
(17) Kinnear, C.; Rodriguez-Lorenzo, L.; Clift, M. J. D.; Goris, B.; Bals, S.; Rothen-Rutishauser, B.; Petri-Fink, A. Decoupling the Shape Parameter to Assess Gold Nanorod Uptake by Mammalian Cells. *Nanoscale* **2016**, *8*, 16416−16426.
(18) Ho, L. W. C.; Yung, W.-Y.; Sy, K. H. S.; Li, H. Y.; Choi, C. K. K.; Leung, K. C.-F.; Lee, T. W. Y.; Choi, C. H. J. Effect of Alkylation on the Cellular Uptake of Polyethylene Glycol-Coated Gold Nanoparticles. *ACS Nano* **2017**, *11*, 6085−6101.
(19) Ji, Z.; Jin, X.; George, S.; Xia, T.; Meng, H.; Wang, X.; Suarez, E.; Zhang, H.; Hoek, E. M. V.; Godwin, H.; Nel, A. E.; Zink, J. I. Dispersion and Stability Optimization of TiO_2 Nanoparticles in Cell Culture Media. *Environ. Sci. Technol.* **2010**, *44*, 7309−7314.
(20) Yang, S.-A.; Choi, S.; Jeon, S. M.; Yu, J. Silica Nanoparticle Stability in Biological Media Revisited. *Sci. Rep.* **2018**, *8*, 185.
(21) Jiang, W.; Hibbert, D. B.; Moran, G.; Herrmann, J.; Jämting, Å. K.; Coleman, V. A. Characterisation of Gold Agglomerates: Size Distribution, Shape and Optical Properties. *RSC Adv.* **2013**, *3*, 7367.
(22) Dobrovolskaia, M. A.; Patri, A. K.; Zheng, J.; Clogston, J. D.; Ayub, N.; Aggarwal, P.; Neun, B. W.; Hall, J. B.; McNeil, S. E. Interaction of Colloidal Gold Nanoparticles with Human Blood: Effects on Particle Size and Analysis of Plasma Protein Binding Profiles. *Nanomedicine* **2009**, *5*, 106−117.
(23) Piella, J.; Bastús, N. G.; Puntes, V. Size-Dependent Protein−Nanoparticle Interactions in Citrate-Stabilized Gold Nanoparticles: The Emergence of the Protein Corona. *Bioconjugate Chem.* **2017**, *28*, 88−97.
(24) Liu, Z.; Zhan, X.; Xu, X.; Wu, Y.; Gu, Z. Static Magnetic Field Dictates Protein Corona Formation on the Surface of Glutamine-Modified Superparamagnetic Iron Oxide Nanoparticles. *Part. Part. Syst. Charact.* **2018**, *35*, 1700418.
(25) Manson, J.; Kumar, D.; Meenan, B. J.; Dixon, D. Polyethylene Glycol Functionalized Gold Nanoparticles: The Influence of Capping Density on Stability in Various Media. *Gold Bull.* **2011**, *44*, 99−105.
(26) Rahme, K.; Chen, L.; Hobbs, R. G.; Morris, M. A.; O'Driscoll, C.; Holmes, J. D. PEGylated Gold Nanoparticles: Polymer Quantification as a Function of PEG Lengths and Nanoparticle Dimensions. *RSC Adv.* **2013**, *3*, 6085−6094.
(27) Uz, M.; Bulmus, V.; Alsoy Altinkaya, S. Effect of PEG Grafting Density and Hydrodynamic Volume on Gold Nanoparticle−Cell Interactions: An Investigation on Cell Cycle, Apoptosis, and DNA Damage. *Langmuir* **2016**, *32*, 5997−6009.
(28) Allen, J. M.; Xu, J.; Blahove, M.; Canonico-May, S. A.; Santaloci, T. J.; Braselton, M. E.; Stone, J. W. Synthesis of Less Toxic Gold Nanorods by Using Dodecylethyldimethylammonium Bromide as an Alternative Growth-Directing Surfactant. *J. Colloid Interface Sci.* **2017**, *505*, 1172−1176.
(29) Kinnear, C.; Dietsch, H.; Clift, M. J. D.; Endes, C.; Rothen-Rutishauser, B.; Petri-Fink, A. Gold Nanorods: Controlling Their Surface Chemistry and Complete Detoxification by a Two-Step Place Exchange. *Angew. Chem., Int. Ed.* **2013**, *52*, 1934−1938.
(30) He, C.; Hu, Y.; Yin, L.; Tang, C.; Yin, C. Effects of Particle Size and Surface Charge on Cellular Uptake and Biodistribution of Polymeric Nanoparticles. *Biomaterials* **2010**, *31*, 3657−3666.
(31) Yue, Z.-G.; Wei, W.; Lv, P.-P.; Yue, H.; Wang, L.-Y.; Su, Z.-G.; Ma, G.-H. Surface Charge Affects Cellular Uptake and Intracellular Trafficking of Chitosan-Based Nanoparticles. *Biomacromolecules* **2011**, *12*, 2440−2446.
(32) Blundell, E. L. C. J.; Healey, M. J.; Holton, E.; Sivakumaran, M.; Manstana, S.; Platt, M. Characterisation of the Protein Corona Using Tunable Resistive Pulse Sensing: Determining the Change and Distribution of a Particle's Surface Charge. *Anal. Bioanal. Chem.* **2016**, *408*, 5757−5768.
(33) Gräfe, C.; Weidner, A.; Lühe, M. V. D.; Bergemann, C.; Schacher, F. H.; Clement, J. H.; Dutz, S. Intentional Formation of a Protein Corona on Nanoparticles: Serum Concentration Affects Protein Corona Mass, Surface Charge, and Nanoparticle−Cell Interaction. *Int. J. Biochem. Cell Biol.* **2016**, *75*, 196−202.
(34) Mottas, I.; Milosevic, A.; Petri-Fink, A.; Rothen-Rutishauser, B.; Bourquin, C. A Rapid Screening Method to Evaluate the Impact of Nanoparticles on Macrophages. *Nanoscale* **2017**, *9*, 2492−2504.
(35) Villiers, C.; Freitas, H.; Couderc, R.; Villiers, M.-B.; Marche, P. Analysis of the Toxicity of Gold Nano Particles on the Immune System: Effect on Dendritic Cell Functions. *J. Nanopart. Res.* **2010**, *12*, 55−60.
(36) Fytianos, K.; Rodriguez-Lorenzo, L.; Clift, M. J. D.; Blank, F.; Vanhecke, D.; von Garnier, C.; Petri-Fink, A.; Rothen-Rutishauser, B. Uptake Efficiency of Surface Modified Gold Nanoparticles Does Not Correlate with Functional Changes and Cytokine Secretion in Human Dendritic Cells *In Vitro*. *Nanomedicine* **2015**, *11*, 633−644.
(37) Morbach, H.; Eichhorn, E. M.; Liese, J. G.; Girschick, H. J. Reference Values for B Cell Subpopulations from Infancy to Adulthood. *Clin. Exp. Immunol.* **2010**, *162*, 271−279.
(38) Bishop, G. A.; Ramirez, L. M.; Baccam, M.; Busch, L. K.; Pederson, L. K.; Tomai, M. A. The Immune Response Modifier Resiquimod Mimics CD40-Induced B Cell Activation. *Cell. Immunol.* **2001**, *208*, 9−17.
(39) Douagi, I.; Gujer, C.; Sundling, C.; Adams, W. C.; Smed-Sörensen, A.; Seder, R. A.; Karlsson Hedestam, G. B.; Loré, K. Human B Cell Responses to TLR Ligands Are Differentially Modulated by Myeloid and Plasmacytoid Dendritic Cells. *J. Immunol.* **2009**, *182*, 1991−2001.
(40) Souwer, Y.; Griekspoor, A.; Jorritsma, T.; de Wit, J.; Janssen, H.; Neefjes, J.; van Ham, S. M. B Cell Receptor-Mediated Internalization of *Salmonella*: A Novel Pathway for Autonomous B Cell Activation and Antibody Production. *J. Immunol.* **2009**, *182*, 7473−7481.
(41) Gustafson, H. H.; Holt-Casper, D.; Grainger, D. W.; Ghandehari, H. Nanoparticle Uptake: The Phagocyte Problem. *Nano Today* **2015**, *10*, 487−510.
(42) Zucker, R. M.; Massaro, E. J.; Sanders, K. M.; Degn, L. L.; Boyes, W. K. Detection of TiO_2 Nanoparticles in Cells by Flow Cytometry. *Cytometry, Part A* **2010**, *77A*, 677−685.
(43) Levine, K. E.; Tudan, C.; Grohse, P. M.; Weber, F. X.; Levine, M. A.; Kim, Y.-S. J. Aspects of Bioanalytical Method Validation for the Quantitative Determination of Trace Elements. *Bioanalysis* **2011**, *3*, 1699−1712.
(44) Sharma, M.; Salisbury, R. L.; Maurer, E. I.; Hussain, S. M.; Sulentic, C. E. W. Gold Nanoparticles Induce Transcriptional Activity of NF-KB in a B-Lymphocyte Cell Line. *Nanoscale* **2013**, *5*, 3747−3756.
(45) Lee, C.-H.; Syu, S.-H.; Chen, Y.-S.; Hussain, S. M.; Aleksandrovich Onischuk, A.; Chen, W. L.; Steven Huang, G. Gold Nanoparticles Regulate the Blimp1/Pax5 Pathway and Enhance Antibody Secretion in B-Cells. *Nanotechnology* **2014**, *25*, 125103.
(46) Dorner, M.; Brandt, S.; Tinguely, M.; Zucol, F.; Bourquin, J.-P.; Zauner, L.; Berger, C.; Bernasconi, M.; Speck, R. F.; Nadal, D. Plasma Cell Toll-like Receptor (TLR) Expression Differs from That of B Cells, and Plasma Cell TLR Triggering Enhances Immunoglobulin Production Introduction. *Immunology* **2009**, *128*, 573−579.
(47) Nicolete, R.; dos Santos, D. F.; Faccioli, L. H. The Uptake of PLGA Micro or Nanoparticles by Macrophages Provokes Distinct *In Vitro* Inflammatory Response. *Int. Immunopharmacol.* **2011**, *11*, 1557−1563.
(48) Silva, A. L.; Peres, C.; Conniot, J.; Matos, A. I.; Moura, L.; Carreira, B.; Sainz, V.; Scomparin, A.; Satchi-Fainaro, R.; Préat, V.; Florindo, H. F. Nanoparticle Impact on Innate Immune Cell Pattern-Recognition Receptors and Inflammasomes Activation. *Semin. Immunol.* **2017**, *34*, 3−24.

(49) Zhu, Q.; Zhang, M.; Shi, M.; Liu, Y.; Zhao, Q.; Wang, W.; Zhang, G.; Yang, L.; Zhi, J.; Zhang, L.; Hu, G.; Chen, P.; Yang, Y.; Dai, W.; Liu, T.; He, Y.; Feng, G.; Zhao, G. Human B Cells Have an Active Phagocytic Capability and Undergo Immune Activation upon Phagocytosis of Mycobacterium Tuberculosis. *Immunobiology* **2016**, *221*, 558−567.
(50) Lichtenstein, D.; Meyer, T.; Böhmert, L.; Juling, S.; Fahrenson, C.; Selve, S.; Thünemann, A.; Meijer, J.; Estrela-Lopis, I.; Braeuning, A.; Lampen, A. Dosimetric Quantification of Coating-Related Uptake of Silver Nanoparticles. *Langmuir* **2017**, *33*, 13087−13097.
(51) Hong, S.; Zhang, Z.; Liu, H.; Tian, M.; Zhu, X.; Zhang, Z.; Wang, W.; Zhou, X.; Zhang, F.; Ge, Q.; Zhu, B.; Tang, H.; Hua, Z.; Hou, B. B Cells Are the Dominant Antigen-Presenting Cells That Activate Naive CD4+ T Cells upon Immunization with a Virus-Derived Nanoparticle Antigen. *Immunity* **2018**, *49*, 695−708.e4.
(52) le Guével, X.; Palomares, F.; Torres, M. J.; Blanca, M.; Fernandez, T. D.; Mayorga, C. Nanoparticle Size Influences the Proliferative Responses of Lymphocyte Subpopulations. *RSC Adv.* **2015**, *5*, 85305−85309.
(53) Saptarshi, S. R.; Duschl, A.; Lopata, A. L. Interaction of Nanoparticles with Proteins: Relation to Bio-Reactivity of the Nanoparticle. *J. Nanobiotechnol.* **2013**, *11*, 26.
(54) Mortimer, G. M.; Butcher, N. J.; Musumeci, A. W.; Deng, Z. J.; Martin, D. J.; Minchin, R. F. Cryptic Epitopes of Albumin Determine Mononuclear Phagocyte System Clearance of Nanomaterials. *ACS Nano* **2014**, *8*, 3357−3366.
(55) Food and Drug Admistration (FDA). Drug Products, Including Biological Products, that Contain Nanomaterials - Guidance for Industry. https://www.fda.gov/downloads/Drugs/GuidanceComplianceRegulatoryInformation/Guidances/UCM588857.pdf (accessed Sep 10, 2018).
(56) Turkevich, J.; Stevenson, P. C.; Hillier, J. A Study of the Nucleation and Growth Processes in the Synthesis of Colloidal Gold. *Discuss. Faraday Soc.* **1951**, *11*, 55.
(57) Zhu, J.; Yong, K.-T.; Roy, I.; Hu, R.; Ding, H.; Zhao, L.; Swihart, M. T.; He, G. S.; Cui, Y.; Prasad, P. N. Additive Controlled Synthesis of Gold Nanorods (GNRs) for Two-Photon Luminescence Imaging of Cancer Cells. *Nanotechnology* **2010**, *21*, 285106.
(58) Michen, B.; Geers, C.; Vanhecke, D.; Endes, C.; Rothen-Rutishauser, B.; Balog, S.; Petri-Fink, A. Avoiding Drying-Artifacts in Transmission Electron Microscopy: Characterizing the Size and Colloidal State of Nanoparticles. *Sci. Rep.* **2015**, *5*, 9793.
(59) Geers, C.; Rodriguez-Lorenzo, L.; Andreas Urban, D.; Kinnear, C.; Petri-Fink, A.; Balog, S. A New Angle on Dynamic Depolarized Light Scattering: Number-Averaged Size Distribution of Nanoparticles in Focus. *Nanoscale* **2016**, *8*, 15813−15821.
(60) Beltran-Villegas, D. J.; Sehgal, R. M.; Maroudas, D.; Ford, D. M.; Bevan, M. A. A Smoluchowski Model of Crystallization Dynamics of Small Colloidal Clusters. *J. Chem. Phys.* **2011**, *135*, 154506.
(61) Technologies Inc. S. Frequencies Cell Types Human Peripheral Blood. https://www.stemcell.com/media/files/wallchart/WA10006-Frequencies_Cell_Types_Human_Peripheral_Blood.pdf (accessed Sep 10, 2018).
(62) Steiner, S.; Mueller, L.; Popovicheva, O. B.; Raemy, D. O.; Czerwinski, J.; Comte, P.; Mayer, A.; Gehr, P.; Rothen-Rutishauser, B.; Clift, M. J. D. Cerium Dioxide Nanoparticles Can Interfere with the Associated Cellular Mechanistic Response to Diesel Exhaust Exposure. *Toxicol. Lett.* **2012**, *214*, 218−225.
(63) U.S. Food & Drug Administration. Elemental Analysis Manual (EAM) for Food and Related Products. http://www.fda.gov/EAM (accessed May 18, 2017).